9th International Conference on Fracture Mechanics of Concrete and Concrete Structures
FraMCoS-9
V. Saouma, J. Bolander, and E. Landis (Eds)
DOI 10.21012/FC9.055

# EXPERIMENTAL AND NUMERICAL ASSESSMENT OF THE SHEAR STRENGTHENING EFFECTIVENESS OF HYBRID COMPOSITE PLATES IN REINFORCED CONCRETE BEAMS

**Hadi Baghi[*], Joaquim A.O. Barros[†], Fatmir Menkulasi[††]**

[*] Louisiana Tech University
Louisiana, USA
e-mail: hadibaghi@gmail.com

[†] University of Minho
Guimaraes, Portugal
e-mail: barros@civil.uminho.pt

[††] Louisiana Tech University
Louisiana, USA
e-mail: fmenkula@latech.edu

**Key words:** Hybrid Composite Plate, CFRP, SHCC, NSM, Numerical Simulation

**Abstract:** This paper presents numerical and experimental studies on the performance of Hybrid Composite Plates (HCPs) as a shear strengthening technique for reinforced concrete (RC) beams. A HCP is a thin plate of Strain Hardening Cementitious Composite (SHCC) reinforced with Carbon Fiber Reinforced Polymer (CFRP) laminates applied according to the Near Surface Mounted technique (NSM). Due to the excellent bond conditions between SHCC and CFRP laminates, these reinforcements provide the necessary tensile strength capacity to the HCP. However, the shear behavior of SHCC material has not been yet fully understood due to lack of an appropriate and accurate direct shear test method. To characterize the behavior of SHCCs in shear, the Iosipescu shear test setup was used to test several specimens, in which the loads were applied in an antisymmetric four point bending configuration to assure a pure shear section. A special geometry for the specimens was chosen to assure a uniform shear stress distribution in the pure shear section. A numerical model is presented for predicting the strengthening effectiveness of HCPs in reinforced concrete beams. The numerical simulations were performed on FEMIX, a computer program that includes a shear crack softening law to simulate the stress transfer mechanism at the shear crack as the crack widens. The values of the parameters that define the shear crack softening law were derived based on simulations of Iosipescu shear tests performed as part of this study. The results of the numerical models for the reinforced concrete beams strengthened with HCPs are compared with the experimental data obtained for this beams. It is demonstrated that the numerical model can predict fairly well the behavior of reinforced concrete beams strengthened with HCPs.

## 1 INTRODUCTION

Strain Hardening Cementitious Composites (SHCCs) are a class of fiber reinforced cement composites (FRCC) that exhibit ductile behavior under tensile loads. They are characterized by a strain hardening response rather than a tension softening response provided by conventional FRCC after crack initiation. The tensile strain hardening phase is accompanied by the formation of a diffused crack pattern of very small crack widths. In recent years, SHCCs have been used in the development of new structural systems and for the rehabilitation of existing structures because of the ability of this material to exhibit a ductile shear behavior, possess high energy absorption capacity, and provide stable hysteretic loops at large drifts [1, 2]. Hybrid Composite Plates (HCPs) have been used primarily to increase the shear capacity of reinforced concrete (RC) beams. A HCP is a thin plate of SHCC that is strengthened by carbon fiber reinforced polymer (CFRP) laminates. Due to the excellent bond conditions between SHCC plate and CFRP laminates, the combination of these components provides the necessary tensile strength capacity to the HCP. Additionally, the high resistance and tensile ductility of SHCCs avoid premature fracture failures in this type of cement composite [3, 4]. However, the shear behavior of SHCC materials have not been fully assessed due to the lack of an accurate and appropriate direct shear test method.

The main difficulty in evaluating the shear strength of this material is developing an accurate test setup capable of introducing a uniform shear stress field. Several shear test setup configurations have been proposed by various researchers [5-9]. One of them is the Iosipescu shear test proposed by Iosipescu (1967) for determining the shear properties of metal and welded joints. This test method was considered appropriate for composite materials, and it was adopted by ASTM D-5379 [10]. The Iosipescu test specimens are loaded in antisymmetric four point bending with a double notch in the region with highest shear force and zero bending moment, which creates a section of pure shear and a uniform shear stress in the reduced section (Figure 1). As shown in Figure 1, the specimen features a depth $h_0$ between two notch roots, an angle α at the notch root, and a notch radius $r$.

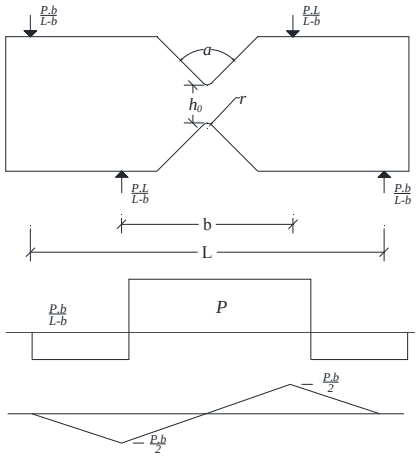


**Figure 1:** Geometry of the notch in the Iosipescu shear test

In this study, the influence of HCPs on the shear strengthening and repairing of RC beam is investigated experimentally and numerically. The shear behavior of the SHCC used in this study is investigated by performing Iosipescu shear tests on ten specimens. The results of these tests are used to derive key parameters needed to develop a shear crack softening law (fracture energy mode II, crack shear strength) for characterizing the behavior of SHCCs in shear. These parameters are then used in numerical simulations of RC beams strengthened with HCPs using a multi-directional fixed smeared crack model available in the FEMIX computer program. This model includes a shear crack softening law to simulate the stress transfer mechanism at the shear crack and the degradation of the shear strength with the widening of the crack [11]. The experimental and numerical results for reinforced concrete beams strengthened with HCPs are compared and it is demonstrated that the numerical model can predict fairly well the behavior of the tested beams.

## 2 SHEAR STRENGHTHENING OF REINFORCED CONCRETE BEAMS

### 2.1 Experimental program

The experimental program consisted of two series of beams. The first series (Series A) is composed of three beams of rectangular cross-section, and the second series (Series B) is formed by five beams of T cross section. Figure 2 shows the monitored shear span of the tested beam. To localize shear failure in only one span, a three point bending test setup of different shear span lengths was adopted. The characteristics of the beams are presented in Table1.

The R-7S-R and T-7S-R beams (Type 1), had $\phi$8@100 mm and $\phi$6@112.5 mm on the monitored shear span, respectively, while the other beams of both series did not include steel stirrups in $L_i$ shear span (Type 2).

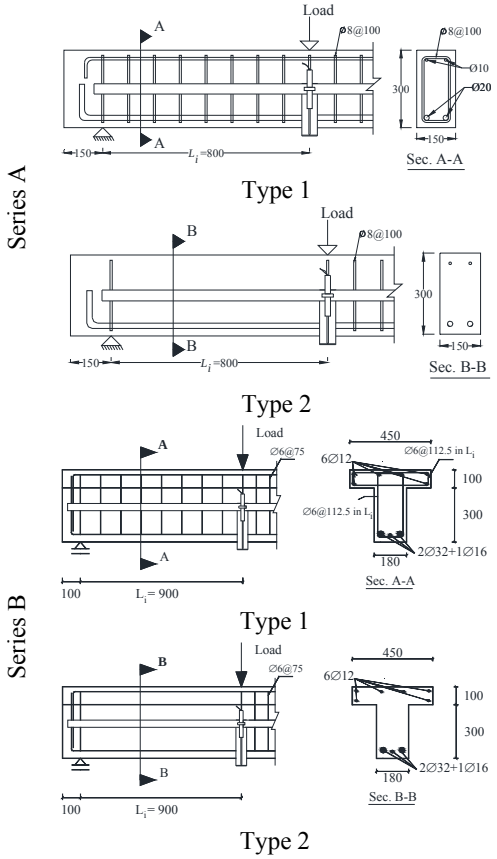


**Figure 1:** Support and loading configuration, geometry and reinforcements of the tested beams (dimensions in mm)

The R-C-R and T-C-R were the control beams without shear reinforcement throughout the $L_i$ span (Type 2). In the first step the control beams were loaded up to failure load, and then fully unloaded. In the next step these beams were repaired by applying the HCPs to each lateral face of the monitored shear span using a combination of epoxy adhesive and mechanical anchors. The repaired beams (Figure 2), designated by R-D-3L and T-D-5L-BC, were subjected to the same test configuration adopted in their undamaged state. In the repaired beams the configuration of the CFRP laminates and mechanical anchors were designed in an attempt of assuring to the HCP the highest resistance to the opening and sliding of existing shear failure crack in the beams to be strengthened.

**Table 1:** Shear strengthening/reinforcement in the monitored shear span of the tested beams

| | Beam designation | Strengthening technique | Spacing, (mm) |
|---|---|---|---|
| A | R-C-R | - | - |
| | R-D-3L | HCPs | 150 |
| | R-7S-R | Steel stirrups | 100 |
| B | T-C-R | - | - |
| | T-5L | HCPs | 157 |
| | T-5L-BC | | |
| | T-D-5L-BC | | |
| | T-7S-R | Steel stirrups | 112.5 |

The T-5L and T-5L-BC (Figure 4) were beams strengthened with HCPs to enhance their shear capacity. To prevent the localization of failure in the web-flange zone, the T-5L-BC and T-D-5L-BC beams were also strengthened with four steel bars connectors that extended from the web into the flange.

The test was conducted in a displacement controlled mode at a rate of 0.01 mm/s. The load was applied using a closed-loop servo controlled hydraulic actuator. The deflection of the beams was measured with one LVDT at the location of the applied load. The material properties of concrete, CFRP laminates, and SHCC are presented in Table 2. The SHCC is composed of a cementitious mortar reinforced with 2% in

volume of short discrete polyvinyl alcohol (PVA) fibers of 40 μm diameter and 8 mm length. The mix composition, curing process and experimental characterization of the SHCC are provided in reference [1]. The average value of the yield stress of the steel bars of 6, 8, 10, 12, 16, 20, and 32 mm diameter was 500, 545, 530, 490, 470, 575, and 625 MPa, respectively, and the average tensile strength was 595, 610, 625, 590, 565, 640, and 905 MPa, respectively.

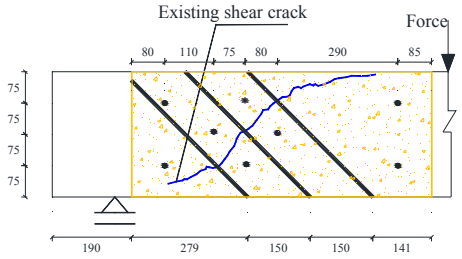


a) R-D-3L

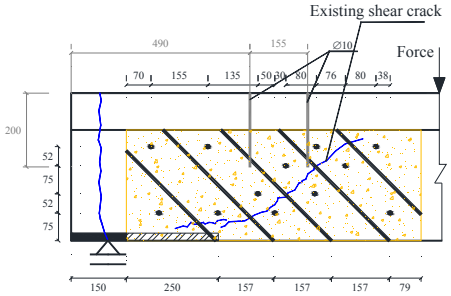


b) T-D-5L-BC

**Figure 2**: Shear strengthening details of repaired beams (dimensions in mm)

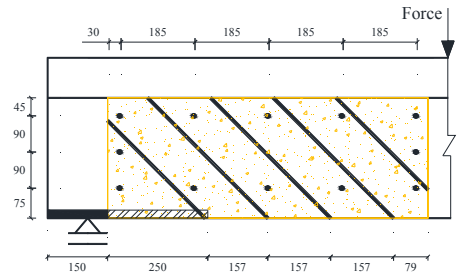


a) T-5L

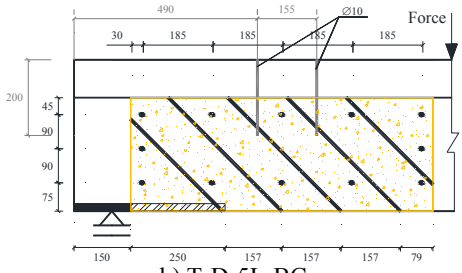


b) T-D-5L-BC

**Figure 3**: Shear strengthening details for tested beams (dimensions in mm)

The HCP in this experimental program was a SHCC plate 20 mm thick that was reinforced with CFRP laminates that were applied according to the NSM technique [12]. More information about the strengthening technique of these beams can be found in [1].

**Table 2:** Material Properties

| Property | Concrete | CFRP | SHCC |
|---|---|---|---|
| Compressive strength (MPa) | 33.0 | - | 32.0 |
| Tensile strength (MPa) | - | 2620 | 3.5 |
| Elasticity modulus (GPa) | - | 150 | 18000 |
| Maximum tensile strain (%) | - | 1.6 | 1.3 |
| Tensile stress at crack initiation (MPa) | - | - | 2.5 |

## 2.2 Results

The relationship between the applied load and deflection for the rectangular and T cross section beams are presented in Figure 5(a) and 5(b), respectively. The maximum load and the corresponding deflection for the tested beams are presented in Table 3. The values for the $F_{max}/F_{max}^{7S-R}$ ratio are also presented in this table, which is the ratio between the maximum load capacity of the beam strengthened with HCPs ($F_{max}$) and its corresponding value in the beam with seven steel stirrups in monitored shear span ($F_{max}^{7S-R}$).

The obtained experimental results show that in the series A, the R-D-3L beams had a maximum load of 88% of the maximum load of the R-7S-R beam, and in the series B the maximum load of the T-5L-BC and T-D-5L-BC beams was 104% and 100% of the T-7S-R beam, respectively.

The R-C-R beam failed in shear with an abrupt drop in the load capacity after the peak load was achieved (Figure 6(a)), the maximum load of this beam was around 45% of maximum load of the corresponding beam with seven steel stirrups in the monitored shear span (R-7S-R beam). The T-C-R beam failed at the support section of the monitored span due

to inadequate anchorage of longitudinal reinforcement (Figure 7a). The maximum load of this beam was around 40% of T-7S-R beam.

The R-7S-R beam failed in bending with the yielding of the flexural reinforcement (Figure 6b). The T-7S-R beam presented a brittle shear behavior, with an abrupt load decay at peak load, which is justified by the relatively high shear reinforcement ratio (Figure 7b).

**Table 3:** Results in terms of load, deflection, and failure mode

| | Beam designation | $F_{max}$ (kN) | Deflection (mm) | $\frac{F_{max}}{F_{max}^{7S-R}}$ (%) |
|---|---|---|---|---|
| A | R-C-R | 81 | 3.3 | 45 |
| | R-D-3L | 161 | 10.1 | 88 |
| | R-7S-R | 182 | 19.9 | 100 |
| B | T-C-R | 214 | 3.0 | 40 |
| | T-5L | 364 | 6.3 | 67 |
| | T-5L-BC | 552 | 9.4 | 104 |
| | T-D-5L-BC | 530 | 7.2 | 100 |
| | T-7S-R | 530 | 8.4 | 100 |

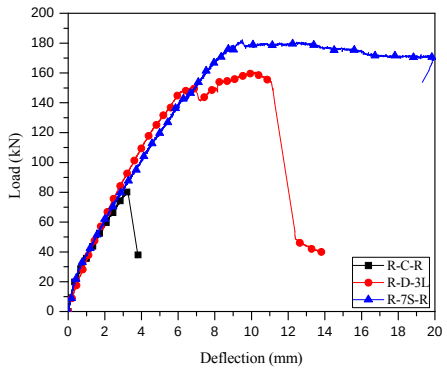


a)

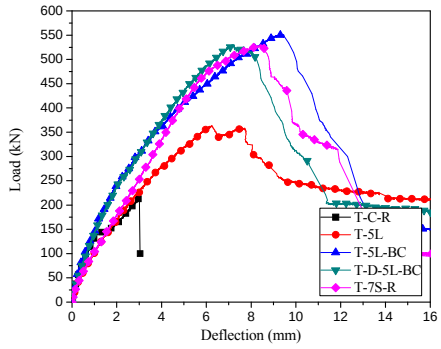


b)

**Figure 5:** Load-deflection at loaded section of series of: a) rectangular cross section, b) T cross section beams

a) R-C-R

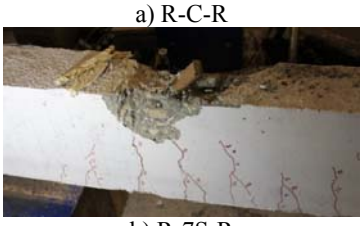

b) R-7S-R

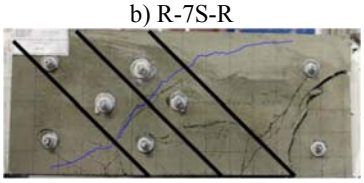

c) R-D-3L

**Figure 6:** Crack pattern at failure load of the rectangular cross section beams

In T-5L beam the HCPs were bonded to the lateral faces of the beams using epoxy adhesive and mechanical anchors. In this beam, the failure was localized at the web-flange zone of the beam. This is due to a strength discontinuity in that area (ellipse in Figure 7c), since no internal stirrups were available to offer resistance to the propagation of this type of failure crack in this zone.

The failure crack of R-D-3L beam was localized in the zone of the HCPs without any CFRP laminate and away from the existing crack (Figure 6c). Due to the excellent bond conditions between SHCC and CFRP laminates, this reinforcement provided the necessary tensile strength capacity to the HCP, while the high post-cracking tensile deformability and resistance of the SHCC avoided the formation of a crack in the vicinity of the existing crack.

To preclude the crack propagation through the web-flange zone (a type of failure observed in the T-5L beam), steel bars were applied to the T-D-5L-BC and T-5L-BC beams as shown in Figures 3b and 4b, respectively. The failure mode in these two beams presents a more diffused crack pattern (Figure 7d and 7e) than in the

previous beams, due to the ability of the bonded and anchored SHCC to preclude the propagation of the existing crack, and to more efficiently contribute in enhancing the shear capacity of the RC beams. The steel bar connectors applied in these beams avoided the occurrence of the premature failure at the web-flange zone, observed in the T-5L beam, and the failure of these beams was governed by shear.

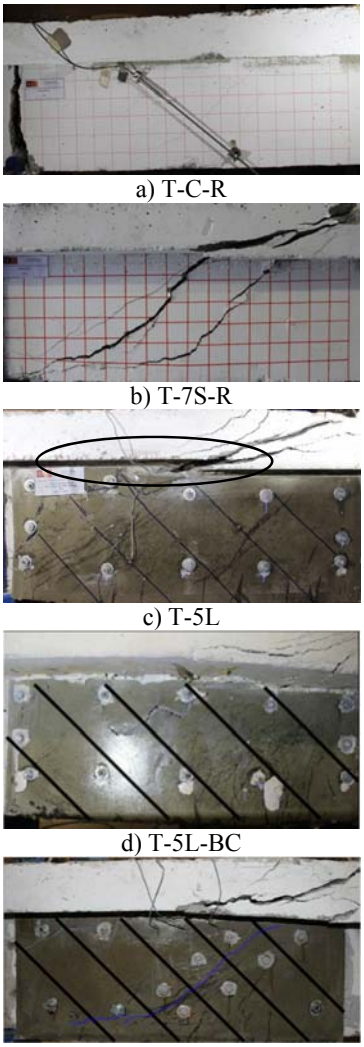

a) T-C-R

b) T-7S-R

c) T-5L

d) T-5L-BC

e) T-D-5L-BC

**Figure 7:** Crack pattern at failure of T cross section beams strengthened with SHCC/HCP

## 3 IOSIPESCU SHEAR TEST:

The main goal of this test is to determine the shear strength at first crack, the relationship between shear stress versus crack sliding of SHCC material, and fracture energy of mode II, $G_{f_s}$. The dimensions of the specimens were 380×140×14.5 mm with depth of the critical cross section ($h_0$) of 25 mm, angle of notch root of ($\alpha$) 90°, and tip radius at notches equal to ($r$) 2.5 mm (Figure 1). The specimen was designed based on the comprehensive studies of Shang and Zijl [13] for finding the geometry of Iosipescu SHCC specimen that assures an uniform shear stress distribution.

### 3.1 Test setup and monitoring system

The test was conducted in a displacement controlled mode at a rate equal to 0.005 mm/s. The load was recorded using a 10 kN load cell. The weight and the slight friction of the movable portion of fixture were taken into account on the evaluation of the strict load applied to the specimen. As shown in Figure 8, one LVDT was installed at the notched section to measure the sliding of the crack.

**Figure 8:** The position of the LVDT to measure the sliding of the shear crack formed in the notched section

### 3.2 Test results and discussion

Ten specimens were tested. The average shear stress was determined by dividing the total applied load (P) (measured by the load cell) by the area of the cross section between the two notches (Eq. 1):

$$\tau_{avg} = \frac{P}{A} \qquad (1)$$

The envelope and the average curve corresponding to the average shear stress versus sliding relationship of the specimens are presented in Figure 9(a). Figure 9(b) shows the typical crack pattern of the specimens.

Iosipescu specimens had similar failure mode and their shear stress-sliding curves denote the existence of three main phases. The first phase corresponds to the linear behavior up to a shear stress of about 0.8 MPa (0.09 mm) and formation of initial vertical cracks. In the second phase, more micro cracks were formed up to peak load. When specimens reached their maximum load, the micro cracks were connected to each other and the load started decreasing (softening stage) up to end of the test (Figure 9(b)). Based on the Figure 9a, for an average slip 2 times the average slip at peak load, the SHCC was still capable of supporting 50% of the average shear strength, which denotes the ductility of this composite material when subjected to shear deformations.

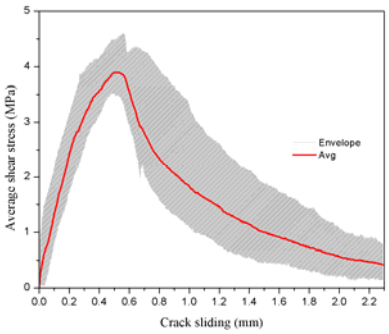


a)

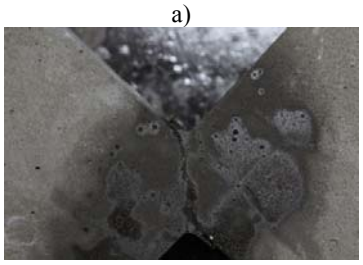

b)

**Figure 9:** a) The envelope and average stress versus crack sliding; b) Typical crack pattern in the tested Iosipescu specimens

By calculating the area under the curve of average shear stress versus sliding after crack initiation (Fig. 10a), the mode II fracture energy of the SHCC material was estimated about 1.4 N/mm, which corresponds to approximately 40% of its mode I fracture energy determined by direct tensile tests with notched specimens.

## 4 NUMERICAL SIMULATION

### 4.1 Numerical simulation of Iosipescu shear test

The two dimensional multi-directional fixed smeared crack model described in [14], implemented in the FEM-based computer program FEMIX [11], is used in the numerical simulations presented herein. To simulate the crack initiation and the fracture mode I propagation of SHCC, the tri-linear tension-softening diagram illustrated in Figure 10 (a) was adopted [14]. The parameters referenced in this diagram are provided in Table 4. This table also includes the data necessary to define the shear-softening diagram that simulates the degradation of crack shear stress after crack initiation [15-17] (Figure 10 (b)). The physical meaning of the remaining variables of this constitutive model can be found elsewhere [15, 16].

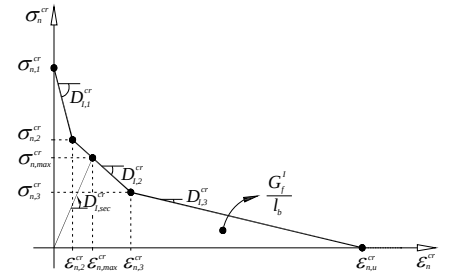


a)

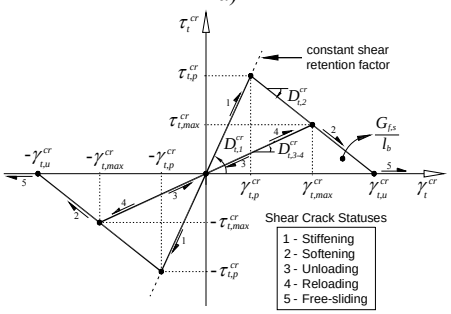


b)

**Figure 10:** a) Tri-linear stress-strain diagram to simulate the fracture mode I crack propagation ( $\sigma_{n,2}^{cr} = \alpha_1 \sigma_{n,1}^{cr}$, $\sigma_{n,3}^{cr} = \alpha_2 \sigma_{n,1}^{cr}$, $\varepsilon_{n,2}^{cr} = \xi_1 \varepsilon_{n,u}^{cr}$, $\varepsilon_{n,3}^{cr} = \xi_2 \varepsilon_{n,u}^{cr}$ ); b) Diagram to simulate the relationship between the shear stress and crack shear strain component, and possible shear crack statuses.

The SHCC used for the Iosipescu beam specimens can be considered to be an

isotropic material due to the random orientation of the short fibers and the relatively small thickness of the Iosipescu beam specimens [13]. In fact, due to the relatively small thickness of the specimens from which the Iosipescu beam specimens are extracted, it is assumed fibers are oriented primarily in the plane. The inverse analysis approach used in simulating the behavior obtained from physical tests allowed the determination of fracture energy mode II and also the shear retention factor.

A comparison between experimental and numerical results in terms the average shear stress and the sliding of the crack at the notched plane is provided in Figure 11a. The numerically predicted crack pattern of the test specimens at the end of the analysis is represented in Figure 11b. The first crack appeared experimentally and numerically at a load of about 0.31 kN and 0.4 kN, respectively and the softening stage started at a load of 1.3 kN and 1.35 kN, respectively. As it is shown in Figure 11, the numerical model is capable of capturing, with acceptable accuracy, the shear behavior of the tested specimens.

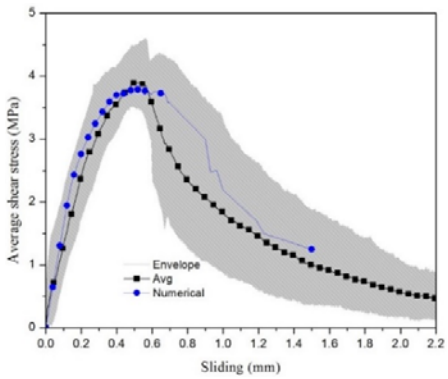


a)

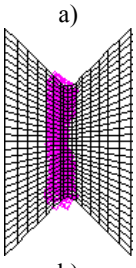

b)

**Figure 11:** a) Comparison between experimental and numerical average shear stress *versus* sliding relationship; b) Crack pattern of the specimens

**Table 4:** Values of the parameters of the SHCC constitutive model

| Parameters | Values |
|---|---|
| $\nu_c$ | 0.15 |
| $E_c\ (N/mm^2)$ | 18000 |
| $f_c\ (N/mm^2)$ | 32.0 |
| $f_{ct}\ (N/mm^2)$ | 2.35 |
| $G_f\ (N/mm)$ | 3.5 |
| $\xi_1$ | 0.11 |
| $\alpha_1$ | 1.27 |
| $\xi_2$ | 0.54 |
| $\alpha_2$ | 0.11 |
| $\tau_{t,p}^{cr}\ (N/mm^2)$ | 1.0 |
| $G_{f,s}\ (N/mm)$ | 1.4 |
| $\beta$ | 0.15 |

## 4.2 Numerical simulation of the tested beams

The three dimensional multi-directional fixed smeared crack model was used in the numerical simulations of the beams. The parameters indicted in Figure 10 (a) and 10 (b) are provided in Table 5 for plain concrete. The data for the shear softening diagram of plain concrete was determined by calibrating the model to match as closely as possible the force-deflection relationship recorded during the control beam test (C-R-I).

The bolts are modeled with 3D two-node truss elements, and the confinement effect locally induced on concrete by the torque of anchors was simulated by applying a temperature decrease of -25.5°C in these elements. More information about the simulations can be found in [1]. To simulate the existing shear crack of the beams to be strengthened, a very small tensile strength and mode I fracture energy was attributed to the finite elements crossing this shear crack. The experimental and numerical results obtained in terms of the applied load and the deflection under the load are compared in Figures 12 and 13.

**Table 5:** Values of the parameters of the concrete constitutive model

| Parameters | Values |
|---|---|
| $\nu_c$ | 0.19 |
| $E_c\ (N/mm^2)$ | 31381 |
| $f_c\ (N/mm^2)$ | 33.0 |
| $f_{ct}\ (N/mm^2)$ | 2.1 |
| $G_f\ (N/mm)$ | 0.08 |
| $\xi_1$ | 0.005 |
| $\alpha_1$ | 0.3 |
| $\xi_2$ | 0.1 |
| $\alpha_2$ | 0.3 |
| $\tau_{t,p}^{cr}\ (N/mm^2)$ | 1.1 |
| $G_{f,s}\ (N/mm)$ | 0.045 |
| $\beta$ | 0.6 |

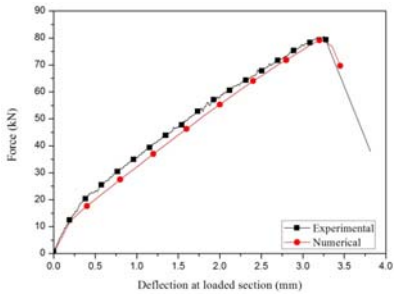


a) R-C-R

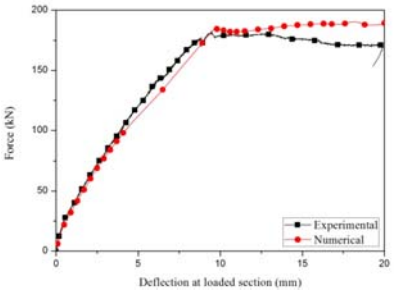


b) R-D-3L

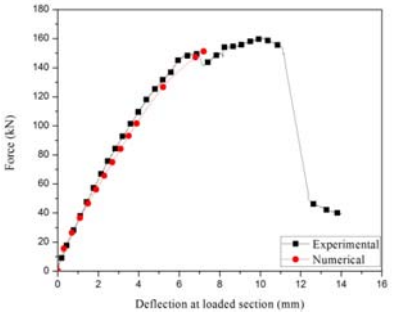


R-7S-R

**Figure 12:** Comparison between experimental and numerical simulation of rectangular beams

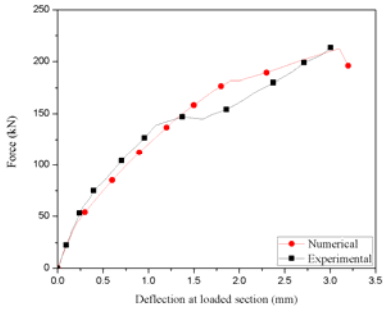


a) T-C-R

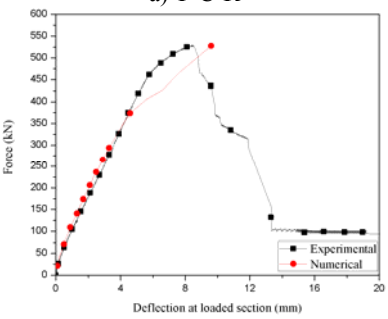


b) T-7S-R

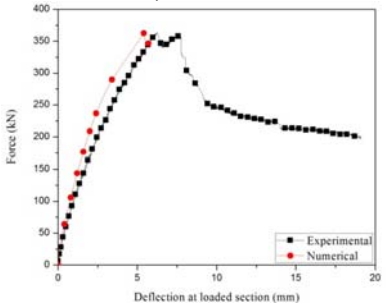


T-5L

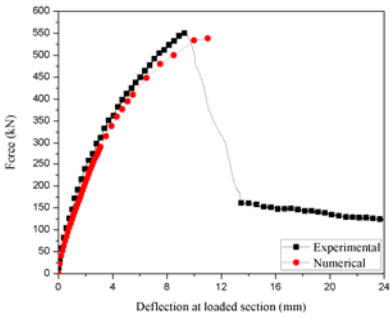


T-5L-BC

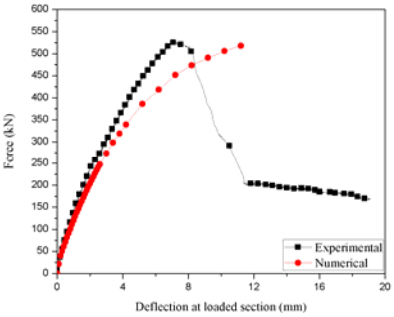


T-D-5L-BC

**Figure 13:** Comparison between experimental and numerical simulation of T cross section beams

The numerical simulations ended at the last converged load increment. The crack patterns of these beams at the end of the analysis are represented in Figures 14 and 15.

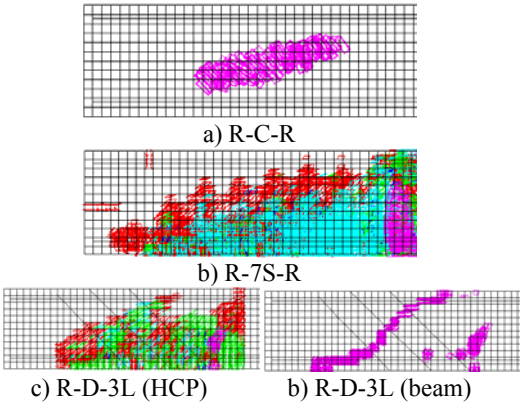


**Figure 14:** Crack pattern of the beams of rectangular cross section

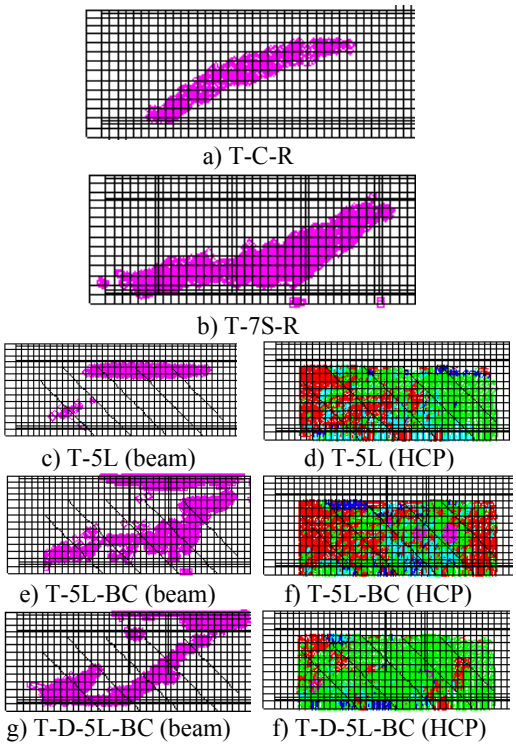


**Figure 15:** Crack pattern of the beams of T cross section

These figures show that the numerical model is capable of predicting with high accuracy the relationship between the load and the deflection of the strengthened and repaired beams. Additionally, the numerical model is fairly accurate in predicting the localization and profile of the cracks at failure. The crack pattern of beam T-5L shows the tendency of the failure crack to propagate at the web-flange interface due to the discontinuity of beam's cross section stiffness and shear strengthening contribution of the HCP. This also justifies the high strengthening contribution of the steel bars applied in the T-5L-BC and T-D-5L-BC beams, since these bars, by crossing this zone, have offered resistance to the propagation of this crack.

## CONCLUSION

The effectiveness of Hybrid Composite Plates (HCPs) for the shear strengthening of pre-damaged reinforced concrete (RC) beams was investigated by carrying out an experimental program. The control beams, without shear reinforcement, were loaded up to their shear failure and then repaired by using HCPs. The localization of the CFRP laminates and mechanical anchors of the HCPs for the strengthening of the damaged beams were designed in order to provide an effective resistance to the propagation of the existing shear crack. The CFRP laminates provided the necessary tensile strength capacity to the HCP, while the high post-cracking tensile deformability and resistance of the SHCC avoids the occurrence of premature fracture failure in this cement composite during the stress transfer process between these two materials when the HCP is crossed by a shear crack.

To demonstrate the efficiency of HCPs in enhancing the shear strength of RC beams, the maximum load of the tested beams was compared to the corresponding beams with steel stirrups in the shear span. The rectangular beam strengthened with HCPs achieved a maximum load of around 88% of the corresponding beam with stirrups in the shear span. The maximum load in the rectangular beam with no strengthening technique and no stirrups in the shear span was 45% of that beam with stirrups in the shear span. Similarly, the maximum load achieved in T-beams strengthened with HCPs varied from 68% to 104% of the corresponding beam with stirrups in the shear span. The maximum load attained

in the T-beam with no strengthening technique and no stirrups was 40% of the maximum load of the beam with stirrups in the shear span. This demonstrates that HCPs can be as efficient as stirrups in enhancing the shear strength of RC beams. Additionally, all beams strengthened with HCPs achieved higher peak loads than the control beams.

The shear behavior of the SHCC was investigated by using Iosipescu shear test method. The shear stress versus sliding curves obtained from this type of test were characterized by three phases: 1) the first phase is characterized by a linear response that ends at an average shear stress of 0.8 MPa and at a sliding of 0.09 mm; 2) the second phase features the development of micro cracks with a continuous decrease of shear stiffness up to peak load (at an average shear strength of 3.9 MPa and sliding of 0.5 mm); and 3) the third phase that exhibits a shear softening behavior due to the degeneration of micro- in macro-cracks in the shear critical region. However, for an average slip 2 times the average slip at peak load the SHCC was still capable of supporting 50% of the average shear strength, which denotes the ductility of this composite material when subjected to shear deformations. By calculating the area under the curve of average shear stress versus sliding, the fracture energy mode II of SHCC material was estimated about 1.4 N/mm, which corresponds to 40% of its mode I fracture energy.

The capability of a FEM-based computer program to predict with high accuracy the shear behavior of SHCC materials and reinforced concrete beams in terms of shear behavior was demonstrated. It was verified that the shear crack softening diagram available in the multi-directional fixed smeared crack model, implemented in the FEMIX computer program, can be used in simulating the shear behavior of the Iosipescu test specimens, and in predicting the load carrying capacity, crack pattern and failure mode of the tested beams.

## ACKNOWLEDGMENTS

The study reported in this paper is part of the project "PrePam –Pre-fabricated thin panels using advanced materials for structural rehabilitation", with the reference PTDC/ECM/114511/2009. The first author acknowledges the grant provided by this project.

## REFERENCE

1. Baghi, H., The effectivness of SHCC-FRP panles of the shear resistance of RC beams, 2015, University of Minho.
2. Baghi, H., Barros, A.O.J., Shear Properties of the Strain Hardening Cementitious Composite Material. Journal of Materials in Civil Engineering (ASCE), 2016. DOI: 10.1061/(ASCE)MT.1943-5533.0001603.
3. Baghi, H., Barros, A.O.J., Shear Strengthening of Reinforced Concrete T Beams with Hybrid Composite Plates (HCPs). Journal of Composites for Construction (ASCE), 2016. DOI: 10.1061/(ASCE)CC.1943-5614.0000693.
4. Baghi, H., Barros, A.O.J., Shear Strengthening of Concrete Beams with Hybrid Composite Plates. Advances in Structural Engineering, 2016. DOI: 0.1177/1369433215622873.
5. Banks-Sills, L., Arcan, M., An Edge Crack Mode II Fracture Specimen. Experimental Mechanics, 1983: p. 257-261.
6. Ohno, K., Shear Tests of Reinforced Concrete Beam by Special Type of Loading. Transactions of the Architectural institute of Japan 1957: p. 581-584.
7. Reinhardt, H.W., Ozbolt, J., Xu, S., Dinku, A., Shear of Structural Concrete Members and Pure Mode II Testing. Advanced Cement Based Materials 1997. 5: p. 75-85.

8. Boulifa, R., M. Laid-Samami, and M. Tayeb benhassine, A New Technique for Studying the Behaviour of Concrete in Shear. Journal of King Saud University, 2013. 25(2): p. 149-159.
9. Iosipescu, N., New accurate method for single shear testing of metals. Journal of Materials, 1967. 3: p. 537-566.
10. (ASTM), A.S.f.T.a.M., ASTM D 5379, Standard Test Method for Shear Properties of Composite Materials by the V-Notched Beam Method, 1993.
11. Sena-Cruz, J.M., Barros, J.A.O., Azevedo, A.F.M., Ventura-Gouveia, A. Numerical simulation of the nonlinear behavior of RC beams strengthened with NSM CFRP strips. in CMNE/CILAMCE Congress, FEUP. 2007. Porto, Portugal.
12. Dias, S.J.E., Barros, J.A.O., Performance of reinforced concrete T beams strengthened in shear with NSM CFRP laminates. Engineering Structures, 2010. 32: p. 373-384.
13. Shang, Q., Zijl, G.V., Characterising the Shear Behaviour of Strain-Hardening Fiber-Reinforced Cement-Based Composites. Journal of the South African Institution of Civil Engineering, 2007. 49: p. 16-23.
14. Sena-Cruz, J.M., Strengthening of concrete structures with near-surface mounted CFRP laminate strips, in Department of Civil Engineering, PhD Thesis,2004, University of Minho.
15. Barros, J.A.O., Baghi, H., Dias, S.J.E.,Ventura-Gouveia. A., A FEM-based model to predict the behaviour of RC beams shear strengthened according to the NSM technique. Engineering Structures, 2013. 56: p. 1192–1206.
16. Ventura-Gouveia, A., Constitutive models for the material nonlinear analysis of concrete structures including time-dependent effects, in Department of Civil Engineering, PhD Thesis,2011, University of Minho.
17. Ventura-Gouveia, A., Barros, J., Azevedo, A., Sena-Cruz, J., Multi-fixed smeared 3d crack model to simulate the behavior of fiber reinforced concrete structures, in CCC 2008 - Challenges for Civil Construction2008: Porto, Portugal.